Proceedings of the 34th European Modeling & Simulation Symposium (EMSS), 014
19th International Multidisciplinary Modeling & Simulation Multiconference

ISSN 2724-0029 © 2022 The Authors.
doi: 10.46354/i3m.2022.emss.014

Modelling of a Multifunction Electromagnetic Interference Shield and Heat Exchanger Device for a Multirotor Drone

Jean-David Wheeler[1*], Nicolas Texier[2], Michelle Malara[1], Thierry Sanlaville[2], Vincent Seconda[2], Vincent Sousselier[2], Jean-Marc Dedulle[1] and Patrick Namy[1]

[1]SIMTEC, 5 rue Félix Poulat, Grenoble, 38000, France
[2]Parrot Drone SA., 174 quai de Jemmapes, Paris, 75010, France

[*]Corresponding author. Email address: jean-david.wheeler@simtecsolution.fr

Abstract

Whereas the processing capacity of multirotor drone increases significantly, the specification applying to the hardware to dissipate the heat becomes more challenging. At the same time, the weight must be reduced, and the electromagnetic vulnerability must still be prevented. In this study, the authors aim at increasing the performance of the drone by taking advantage of new material properties and a science-based approach. A numerical model of the heat transfers in the drone is developed using COMSOL Multiphysics®. Moreover, two specific analytical models from the literature are identified and solved to predict the shield performance. Thanks to the physic predictions, it is possible to determine the minimum material quantity to achieve the best performances. Design guidelines are derived for the engineers to develop the next generation of multirotor drones.

Keywords: Electromagnetic shield; heat; lightweight; magnesium; drone

1. Introduction

Parrot is the European leader in the design of lightweight multirotor drones (mass less than 1kg). These drones are small computers embedded on a flying structure. The control is deported to a remote control, via a radio link. Electronic boards hosting computing capabilities must be encapsulated to reduce electromagnetic interactions (Kim et al., 2019; Li et al., 2021; Mach et al., 2017; Mendoza-Mendoza et al., 2021) (defined by certification constraint and RF environmental pollution detrimental to the control link). Besides, the heat inherent in this type of circuit must be extracted (García Barreras, 2015; Mendoza-Mendoza et al., 2021). Traditionally this is done via the superposition of shielding and radiator (Mendoza-Mendoza et al., 2021). However, this solution has the double disadvantage of being heavy, of a significant volume, and especially less efficient from a thermal point of view because of the multiplication of interfaces. Improved design requires to hunt for unnecessary parts and group several functions on one part. This paper investigates the possibility to use a magnesium radiator to close the shield. The study is led by Parrot and SIMTEC is responsible for modelling the behavior of a magnesium part for both thermal aspects and shielding to validate the concept and establish sizing rules.

2. Materials and methods

2.1. Geometry

An analysis of the multirotor drone designs shows that different layers are involved. In the drone main body, the heat is mainly emitted by the chips. Both the heat path and the electromagnetic shielding is achieved by the superposition of different layers and junction pastes.

Since the chip, the shield and the radiator all have one dimension much smaller than the other ones, the study is led on an equivalent 1D geometry (see Figure 1) where only the thickness of the different layers is represented.

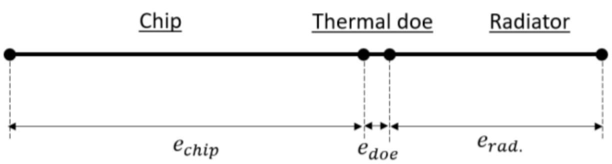

Figure 1. One dimension geometry with the different thicknesses of the layers

The cross-section area retained is $A_c = 25\ cm^2$.

2.2. Heat transfer numerical model

To predict the temperature rise in the device for a given operating condition, one must solve the heat transfer equation and the appropriate boundary condition. The heat transfer equation reads:

$$\frac{\partial}{\partial x}\left(-A_c k \frac{\partial T}{\partial x}\right) = A_c Q \tag{1}$$

with x the spatial variable, k the conductivity of the material, T the temperature and Q the heat source in the chip. On the chip side the boundary condition is an insulation:

$$-A_c k \frac{\partial T}{\partial x} = 0 \tag{2}$$

And on the radiator side the boundary condition is a heat flux:

$$-A_c k \frac{\partial T}{\partial x} = h \cdot (T - T_{ext}) \tag{3}$$

with h the heat transfer coefficient (which aggregates convection and radiation cooling) and T_{ext} the external temperature. The heat transfer coefficient can take different values depending on the air flow velocity, and the external temperature is set at 40°C as a reference case.

2.3. Electromagnetism numerical model

In the present study, the frequencies of interest range from 100MHz to 5 GHz and any electromagnetic wave beyond the shield is prohibited. Therefore, there is no point including the drone components apart from the shield itself. However, two potential weaknesses are identified:

- The electromagnetic power density able to cross the shield
- The power able to cross local openings in the shield system.

Two different approaches are used to evaluate the two weaknesses and prevent them.

2.3.1. *Flat shield model*

The physics model aims at solving the Maxwell equations (J. C. Maxwell, 1873) in the present context. It starts with the identification of the index of refraction n for metals which is, according to Feynman (Leech, 1966):

$$n^2 = 1 + \frac{\sigma/\epsilon_0}{i\omega(1 + i\omega\tau)} \tag{4}$$

with σ the conductivity, ϵ_0 the permittivity of vacuum, ω the pulsation, $\tau = \frac{m\sigma}{Nq_e}$ the average time between free collisions of a free electron, N the number of electrons, m the mass of an electron, and q_e the charge of an electron. For low frequencies ($f < 10^{12} Hz$ in a metal), it can be approximated by:

$$n^2 = -i\frac{\sigma}{\epsilon_0\omega} \tag{5}$$

which is further derived into the real n_R and imaginary n_I parts:

$$n_R = \sqrt{\frac{\sigma}{2\epsilon_0\omega}} \text{ and } n_I = i\sqrt{\frac{\sigma}{2\epsilon_0\omega}} \tag{6}$$

Let the magnetic field:

$$H_z = H_0 e^{-\omega n_I x/c} e^{i\omega(t - n_R x/c)} \tag{7}$$

with x the depth axis, z the transverse direction and c the light velocity in the vacuum. By combining (6) and (7), the magnetic field reads:

$$H_x = H_0 e^{-z/\delta} e^{i\omega t - iz/\delta} \tag{8}$$

with $\delta = \sqrt{\frac{2}{\sigma\mu\omega}}$ the skin depth. Starting from the basics and neglecting the surface roughness (E. Maxwell, 1947), it is clear that the classical skin depth equation and the exponential decay with the thickness applies in the present case, as in (Sun et al., 2016).

2.3.2. *Hole model*

Let's consider a small circular hole (diameter d) in a perfect conductor. After (Bethe, 1944) it is possible to estimate the attenuation A of the field using the expression:

$$A = \left(\frac{d}{\lambda}\right)^2 \tag{9}$$

with λ the wavelength.

2.4. Mesh

Since the models for electromagnetism phenomena are purely analytical, no discretization is required. The heat transfer equation and its boundary condition require a mesh as the finite element method is used. A minimum of 10 linear Lagrange elements are used in the thickness of each layer, providing an easy to solve equation system and a low discretization error.

2.5. Materials

The different material properties involved are listed in the present section.

Table 1. Material table.

Material	$k\ [W/(m \cdot K)]$	$\sigma\ [S/m]$	$\mu_r[-]$	$d\ [kg/m^3]$
NiCu	-	$3.58 \cdot 10^6$	1	8730
Magnesium	72	$6.38 \cdot 10^7$	1	1810
Chip	148	-	-	-
Thermal doe	300	-	-	-

2.6. Solver

Because the electromagnetism topic is treated analytically, tables are created to show the shield thickness to get $-80dB$ or the shield weight to get $-80dB$, depending on the frequency and the shielding materials, NiCu and Magnesium.

Contrarily, the heat transfer question requires a more advanced numerical analysis with a linear solver. COMSOL Multiphysics® is used to perform the computations and the post-treatment.

In both cases, the computation time is below consideration level.

3. Results

3.1. Maximum temperature in the chip

Because the cooling method is not completely determined, the heat transfer coefficient h is considered as a parameter. The heat transfer is solved for a magnesium radiator. In Figure 2, the temperature gradient is imperceptible for a given configuration: this emphasis the key role of the heat transfer coefficient at the heat flux boundary. Depending on this coefficient, the temperature ranges between almost 40°C and almost 300°C. The temperature results are in accordance with the experiments led by Parrot team. The design guidelines stemming from this numerical set of results are presented in the discussion section.

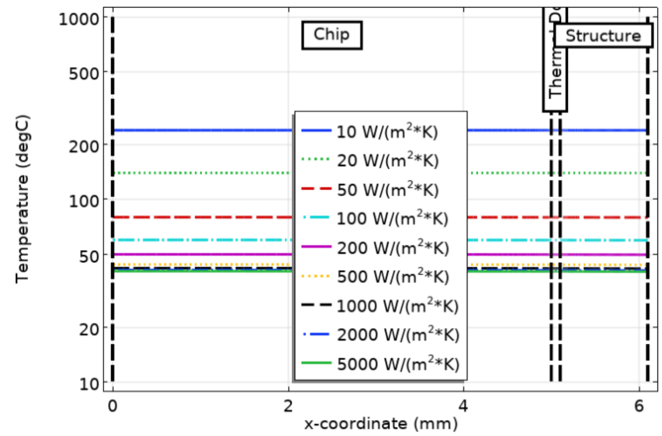

Figure 2. Temperature in the layered material depending on the heat transfer coefficient

3.2. Shield minimum thickness

Thanks to the equation (8) it is possible to compute the electromagnetic wave intensity decay in the metal. The aim is to reach an attenuation of 80 dB while crossing the shield. The results are therefore presented as the minimum thickness to obtain such a performance in Table 2.

Table 2. Minimum shield thickness [μm] to obtain -80 dB

Material	0.1 GHz	0.7 GHz	5 GHz
NiCu	26.6	10.1	3.8
Magnesium	18.9	7.5	2.8

Table 2 results are in very close agreement to the measurements conducted by Parrot team and confirm the numerical approach.

The two materials have different densities, and the actual goal is to minimize the weight of the quadcopter. Table 3 presents the same results using the minimum surface density to achieve the same 80 dB attenuation.

Table 3. Minimum shield surface density [g/m²] to obtain -80 dB

Material	0.1 GHz	0.7 GHz	5 GHz
NiCu	4280	1618	605
Magnesium	664	251	94

3.3. Hole maximum size

Depending on the considered frequency and the hole diameter, the attenuation predicted by (Bethe, 1944) formula varies importantly. The results are summarized in Table 4.

Table 4. Attenuation (dB) depending on the frequency and the hole diameter

Hole diameter [μm]	0.1 GHz	0.7 GHz	5 GHz
1	-135.6	-118.7	-101.6
10	-115.6	-98.7	-81.6
100	-95.6	-78.7	-61.6
1000	-75.6	-58.7	-41.6

4. Discussion

The main question is the replacement of a previous assembly made of a radiator and a NiCu shield by a single Magnesium radiator. In 3.1, it was demonstrated that the key factor for cooling is the heat transfer coefficient: indeed, the temperature gradient is negligible in all the considered layers even thought their properties are rather different. As a result, concentrating the shielding and cooling functions on a single part is likely to reduce the weight without influencing the cooling itself: instead, the design effort should focus on the cooling method and the radiator surface exchange to reduce the temperature in the device.

Thanks to the results presented in 3.2 and 3.3 different design guidelines can be identified. Whether the shielding is insured by a NiCu or a Magnesium metal layer, very thin sheets (a few 1/100 mm only) create a significant protection. Moreover, the magnesium is more conductive than the NiCu alloy considered, and its shielding ability is better. The improvement is even more significant when weight comes into play. The lower density of Magnesium allows a similar shielding effect as NiCu with approximately 7 times less weight. Unfortunately, the conclusions pertaining to the attenuation through a hole are less clear. Under the perfect conductor assumption, a 10µm hole diameter is decreasing the wave intensity by at least 80dB. However, the perfect conductor hypothesis is not fully fulfilled by metals and even less fulfilled if the seal properties are involved. The attenuation is likely to be less important with resistive materials. Whereas trends can be identified with (Bethe, 1944) approach, the analysis must be completed by experimental considerations.

5. Conclusion

Thanks to a robust analysis in two physic domains, the evolution of quadcopter drone design is assessed against science-based predictions. Replacing two components by one leverage weight savings and simplifies the heat path. This can be done without compromising the electromagnetic shielding abilities of the system if designed correctly. Whereas a very thin layer of magnesium can achieve an important wave intensity decay, the designers should focus their attention on reducing the size of the imperfections leading to holes at the junction between the shield parts. This can be done by estimating the hole size impact and leading appropriate measurements on the device.

This study shows that an appropriate modelling of the physics phenomena can provide very tangible design guidelines, thus reducing the iterations in a trial-and-error approach and the global time to market.

Acknowledgements

The authors would like to thank the Parrot company for funding the study and allow for publishing some of the results in the present document.

References

Bethe, H. A. (1944). Theory of Diffraction by Small Holes. *Physical Review*, *66*(7–8), 163. https://doi.org/10.1103/PhysRev.66.163

García Barreras, C. (2015). *Design of a quadcopter to work at high temperatures* [Universidad Carlos III de Madrid]. https://e-archivo.uc3m.es/handle/10016/26822

Kim, S., Noh, Y. H., Lee, J., Lee, J., Choi, J. S., & Yook, J. G. (2019). Electromagnetic Signature of a Quadcopter Drone and Its Relationship with Coupling Mechanisms. *IEEE Access*, 7, 174764–174773. https://doi.org/10.1109/ACCESS.2019.2956499

Leech, J. W. (1966). The Feynman lectures on physics. In *Physics Bulletin* (Vol. 17, Issue 10). IOP Publishing. https://doi.org/10.1088/0031-9112/17/10/010

Li, Y., Ding, Q., Li, K., Valtchev, S., Li, S., & Yin, L. (2021). A Survey of Electromagnetic Influence on UAVs from an EHV Power Converter Stations and Possible Countermeasures. *Electronics 2021, Vol. 10, Page 701*, *10*(6), 701. https://doi.org/10.3390/ELECTRONICS10060701

Mach, V., Kovář, S., Valouch, J., Adámek, M., & Silva, R. M. S. (2017). Threshold levels of electromagnetic susceptibility for unarmed air vehicles. *Progress in Electromagnetics Research Symposium*, *2017-November*, 2483–2488. https://doi.org/10.1109/PIERS-FALL.2017.8293553

Maxwell, E. (1947). Conductivity of metallic surfaces at microwave frequencies. *Journal of Applied Physics*, *18*(7), 629–638. https://doi.org/10.1063/1.1697818

Maxwell, J. C. (1873). *A Treatise on Electricity and Magnetism : vol1* (Clarendon Press Series (Ed.)). Macmillan and co.

Mendoza-Mendoza, J. A., Gonzalez-Villela, V. J., Aguilar-Ibañez, C. F., & Fonseca-Ruiz, L. (2021). Drone Design Concepts. *Drones to Go*, 1–38. https://doi.org/10.1007/978-1-4842-6788-2_1

Sun, J., Wang, W., & Yue, Q. (2016). Review on Microwave-Matter Interaction Fundamentals and Efficient Microwave-Associated Heating Strategies. *Materials 2016, Vol. 9, Page 231*, 9(4), 231. https://doi.org/10.3390/MA9040231